Dyes and Pigments 191 (2021) 109363

Contents lists available at ScienceDirect

Dyes and Pigments

journal homepage: http://www.elsevier.com/locate/dyepig

Peroxide-responsive boronate ester-coupled turn-on fluorogenic probes: Direct linkers supersede self-immolative linkers for sensing peroxides

Abu Sufian [a], Debojit Bhattacherjee [a,b], Tripti Mishra [a], Krishna P. Bhabak [a,b,*]

[a] Department of Chemistry, Indian Institute of Technology Guwahati, Guwahati, 781039, Assam, India
[b] Centre for the Environment, Indian Institute of Technology Guwahati, Guwahati, 781039, Assam, India

ARTICLE INFO

Keywords:
Boronate ester
ROS
Peroxide
Sensor
Self-immolative linker
Turn-on fluorescence

ABSTRACT

Turn-on fluorogenic probes are commonly utilized for an efficient estimation of reactive oxygen species such as H_2O_2. In the present study, three different sets of turn-on fluorogenic probes for sensing H_2O_2 were rationally designed by coupling boronate ester group with three important fluorescent dyes either by linking directly or *via* self-immolative linkers. Interestingly, our results reveal that directly-linked boronate ester probes are superior and sensitive than the self-immolative linker-containing probes in detecting traces of exogenous and endogenous levels of H_2O_2. The difference in probe efficiency was also dependent on the nature of fluorophore unit being used. Considering these aspects, our detailed studies reveal that the directly-linked boronate ester-based fluorescein probe **19** is the best probe for efficiently sensing H_2O_2 both in aqueous as well as cellular medium with very high level of sensitivity. The present observation would be useful while designing the fluorogenic sensors for ROS as well as during their utilization in ROS-associated pathologies.

1. Introduction

Hydrogen peroxide (H_2O_2) is an important non-radical oxidant among reactive oxygen species (ROS), which is produced enzymatically in the mammalian system by the metabolism of molecular oxygen [1]. An overproduction of H_2O_2 has been implicated as the hallmark of oxidative stress in several pathological conditions as well as disease states and therefore, it is extremely important to estimate the endogenous level of H_2O_2 under normal and pathological conditions [2–6]. Use of turn-on fluorogenic probes containing H_2O_2-reactive group(s) has been shown as very useful non-invasive and sensitive tools for monitoring the endogenous level of H_2O_2 in living systems and for ROS-triggered drug delivery under a particular disease condition [7]. Despite the use of various ROS-sensitive groups in ROS-sensors or ROS-mediated drug delivery vehicles, boronate esters are utilized extensively since last two decades for its enhanced selectivity towards H_2O_2 over the other oxidants in ROS family [8–12]. First boronate ester-coupled turn-on fluorogenic probe with a self-immolative carbamate linkage to aminocoumarin was developed by Lo and co-workers in 2003 [13]. In 2004, Chang's group reported the first directly-linked boronate ester probe by utilizing both the hydroxyl groups in fluorescein (probe **1**, Table S1, ESI) [14]. Since then a number of H_2O_2-sensitive probes are being reported by them or by other research groups by coupling the boronate ester group with different fluorescent dyes (Table S1, Supplementary information section). In most of the turn-on fluorogenic probes for sensing H_2O_2 or H_2O_2-meidated drug delivery, the boronate ester group was linked to the fluorophore unit using two main strategies namely-i) direct installation on to the aromatic nuclei in place of –OH group (probes **1**, **2**, **7** and **13**) [14–17]; ii) coupling of self-immolative boronate benzyl group with the –OH or $–NH_2$ group on aromatic nuclei *via* an ether (probes **5**, **6**, **9**–**11** and **14**) [18–23] or carbonate/carbamate (probes **3**, **4**, **8** and **12**) [24–27] linkage (Scheme 1).

The active fluorophore is released in the second strategy upon the reaction with H_2O_2 followed by self-immolation process *via* quinone methide (QM) intermediates as shown in Scheme 1A. The first ether-linked turn-on probe **5** was reported by Cohen and co-workers in 2013, considering the synthetic ease and aqueous stability of the probe [18] and the strategy was used further for H_2O_2 sensing and H_2O_2-mediated drug delivery. Considering the H_2O_2-responsive directly-linked or self-immolative boronate ester-containing probes reported till date, there are few observations-i) coupling strategies (direct *vs* self-immolative) were mostly made randomly or by considering synthetic ease and aqueous stability without analysing their sensitivity

* Corresponding author. Department of Chemistry, Indian Institute of Technology Guwahati, Guwahati, 781039, Assam, India.
E-mail address: kbhabak@iitg.ac.in (K.P. Bhabak).

https://doi.org/10.1016/j.dyepig.2021.109363
Received 29 January 2021; Received in revised form 24 March 2021; Accepted 29 March 2021
Available online 3 April 2021

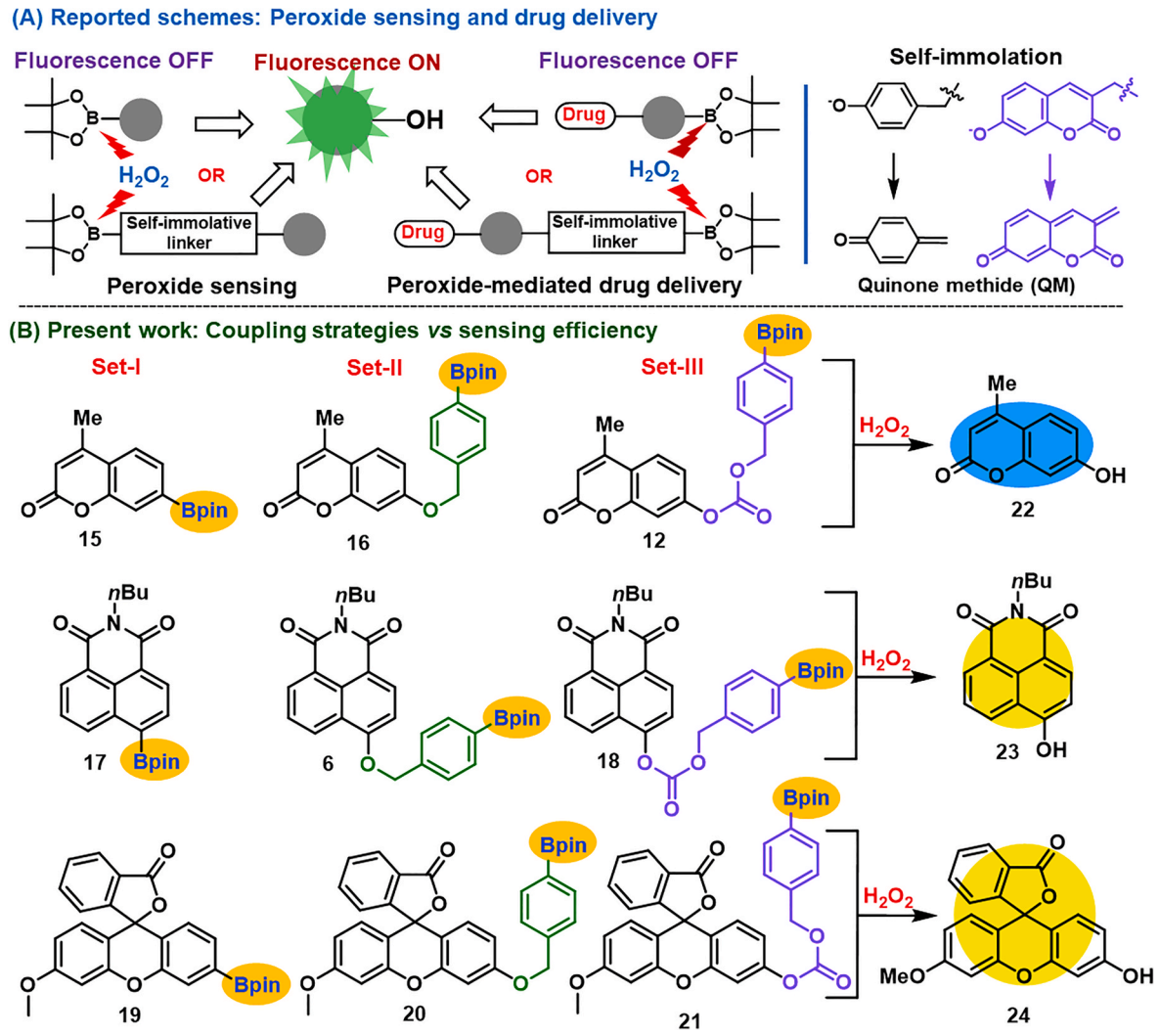

Scheme 1. (A) Reported schemes for H_2O_2-sensing and H_2O_2-mediated drug delivery. (B) Chemical structures of the designed turn-on fluorogenic probes with three different types of boronate ester linkers and the schematic representation for fluorophore release in the presence of H_2O_2.

towards the analyte; ii) absence of comparative data while reporting a new probe with different coupling strategies; iii) incidentally, several of the reported probes are not sensitive enough to detect the endogenous level of H_2O_2 in cellular medium and thus external addition of H_2O_2 or H_2O_2-inducer were necessary for fluorescence turn-on [28,29]. However, a proper rationalization is essential not only for the synthetic ease and stability of the probe, but for the sensitivity and reactivity of the probe towards the analyte of interest (H_2O_2). Therefore, concerning the above drawbacks and to understand and identify the suitable coupling strategies of boronate ester groups with fluorophore units in H_2O_2-responsive probes, we have rationally designed possible combination of boronate ester-based probes using three different and well-known fluorophores (**22**–**24**) covering a wide emission spectral range (Scheme 1).

Herein, we report for the first time that, directly-linked boronate ester probes are significantly more sensitive and reactive towards H_2O_2 than the probes with self-immolative linkers under both of aqueous and cellular environments, making them as best candidates for sensing traces of exogenous and endogenous H_2O_2. Furthermore, the marked selectivity of directly-linked probes over the self-immolative probes was also dependent on the nature of fluorophore used and probably associated with their relative reactivities.

2. Experimental section

2.1. Materials and methods

All the chemicals and solvents were purchased either from Sigma Aldrich, Merck or from reputed local suppliers. All the solvents were either distilled or dried following standard method before using in reactions and chemicals were used without further purification. Thin layer chromatographic (TLC) analyses were carried out on pre-coated silica gel on aluminium sheets and the compounds were visualized by irradiation with UV (254 nm) or fluorescent light (366 nm) and stained by iodine. Organic solvents used for chromatographic separations were distilled before use. Melting point of the synthesized compounds were recorded in a Büchi B540 melting point apparatus and the values are uncorrected. The NMR spectra were recorded with a Bruker Ascend ™ 400 MHz and 600 MHz NMR Spectrometers. Chemical shifts are cited with respect to Me_4Si as internal standard. Mass spectra were obtained using an Agilent 6520 Accurate- Mass Quadrupole Time-of-Flight (Q-TOF) LC/MS spectrometer. The compounds **23** and **24** were synthesized following the reported procedures [30,31].

2.2. Synthesis of the probes

Synthesis of compound 15 [32]: To a stirred solution of compound

33 (0.40 g, 1.29 mmol) and bis(pinacolato)diboron (0.60 g, 2.59 mmol) in 1,4-dioxane (20 mL) was sequentially added $Pd(dppf)Cl_2$ (0.10 g, 0.13 mmol) and KOAc (0.40 g, 3.89 mmol) under argon atmosphere at room temperature. The reaction mixture was stirred at 85 °C for 12 h. Upon completion, the solvent was evaporated under reduced pressure and the residue was diluted with ethyl acetate (20 mL). The reaction mixture was filtered through Celite bed to remove undesired materials and washed with ethyl acetate (3 × 20 mL). The combined organic layer was washed with water and brine (3 × 20 mL). The organic layer was dried over anhydrous sodium sulfate and concentrated under reduced pressure to afford the crude compound. The crude product was purified by silica gel column chromatography using 20% ethyl acetate in pet ether to afford the pure product **15** as white solid. $R_f = 0.5$ (25% ethyl acetate in pet ether). Yield: 0.38 g (89%); M.P. = 145–147 °C. ^{1}H-NMR ($CDCl_3$, 400 MHz): δ (ppm) = 7.74 (s, 1H), 7.69 (d, $J = 7.8$ Hz, 1H), 7.58 (d, $J = 7.8$ Hz, 1H), 6.33 (d, $J = 1.1$ Hz, 1H), 2.45 (d, $J = 1.1$ Hz, 3H), 1.37 (s, 12H). ^{13}C NMR (100 MHz, $CDCl_3$) δ (ppm): 160.8, 152.9, 152.0, 130.0, 123.7, 123.0, 122.0, 116.1, 84.4, 24.9, 18.6. ESI-MS (+ve) *m/z* calcd for $C_{16}H_{19}BO_4$ $[M + H]^+$: 287.1455; found: 287.1455.

Synthesis of compound 16: To a stirred solution of compound **22** (0.20 g, 1.13 mmol) in anhydrous DMF (0.5 ml) was added K_2CO_3 (0.10 g, 1.70 mmol) under argon atmosphere at 0 °C and the mixture was stirred for 1 h. A solution of compound **31** (0.20 g, 1.36 mmol) in anhydrous DMF (0.5 mL) was added dropwise to the reaction mixture and the mixture was stirred at room temperature for 12 h. Upon completion, the reaction mixture was diluted with ethyl acetate (50 mL) and washed with water and brine (3 × 10 mL). The organic layer was dried over anhydrous sodium sulfate and concentrated under reduced pressure to afford the crude residue. The crude product was purified by flash chromatography using 20% ethyl acetate in pet ether to afford the pure product **16** as white solid. $R_f = 0.5$ (20% ethyl acetate in pet ether). Yield: 0.19 g (85%); M.P. = 192–194 °C. ^{1}H-NMR ($CDCl_3$, 400 MHz): δ (ppm): 7.84 (d, $J = 7.9$ Hz, 2H), 7.49 (d, $J = 8.8$ Hz, 1H), 7.43 (d, $J = 7.8$ Hz, 2H), 6.93 (dd, $J_1 = 8.8$ Hz, $J_2 = 2.4$ Hz, 1H), 6.87 (d, $J = 2.4$ Hz, 1H), 6.14 (s, 1H), 5.15 (s, 2H), 2.39 (s, 3H), 1.35 (s, 12H). ^{13}C NMR (100 MHz, $CDCl_3$) δ (ppm): 161.6, 161.2, 155.2, 152.5, 139.0, 135.2, 126.6, 125.6, 113.8, 112.9, 112.1, 102.0, 83.9, 70.4, 24.8, 18.6. ESI-MS (+ve) *m/z* calcd for $C_{23}H_{25}BO_5$ $[M + H]^+$: 393.1873; found: 393.1880.

Synthesis of compound 12: To a stirred solution of compound **22** (0.13 g, 0.75 mmol) and triethylamine (0.20 mL, 1.50 mmol) in anhydrous DCM (5 mL), the solution of compound **32** (0.20 g, 0.50 mmol) in anhydrous DCM (3 mL) was added in a dropwise manner at ice-cold condition under argon atmosphere and the reaction mixture was allowed to attain room temperature and stirred for 24 h. Upon completion, the reaction mixture was diluted with DCM (50 mL) and sequentially washed with saturated $NaHCO_3$ solution, water and brine solution (3 × 10 mL). The organic layer dried over sodium sulfate and evaporated under reduced pressure to afford the crude product, which was purified by flash chromatography using 10% ethyl acetate in pet ether to afford the pure product **12** as white solid. $R_f = 0.5$ (20% ethyl acetate in pet ether). Yield: 0.11 g (64%); M.P. = 140–141 °C. ^{1}H-NMR ($CDCl_3$, 600 MHz): δ (ppm): 7.85 (d, $J = 7.9$ Hz, 2H), 7.61 (d, $J = 8.7$ Hz, 1H), 7.45 (d, $J = 7.9$ Hz, 2H), 7.23 (d, $J = 2.3$ Hz, 1H), 7.17 (dd, $J_1 = 8.7$ Hz, $J_2 = 2.3$ Hz, 1H), 6.28 (d, $J = 0.9$ Hz, 1H), 5.31 (s, 2H), 2.44 (d, $J = 1.0$ Hz, 3H), 1.36 (s, 12H). ^{13}C NMR (100 MHz, $CDCl_3$) δ (ppm): 160.4, 154.1, 153.2, 152.8, 151.9, 137.2, 135.1, 127.6, 125.5, 118.0, 117.3, 114.7, 110.0, 84.0, 70.7, 24.9, 18.7. ESI-MS (+ve) *m/z* calcd for $C_{24}H_{25}BO_7$ $[M + H]^+$: 437.1772; found: 437.1772.

Synthesis of compound 17: To a mixture of bis(pinacolato)diboron (0.60 g, 2.25 mmol) and compound **34** (0.25 g, 0.75 mmol) in anhydrous 1,4-dioxane (20 mL) was added $Pd(dppf)Cl_2$ (55 mg, 0.07 mmol) and KOAc (0.18 g, 2.25 mmol) under argon atmosphere at room temperature. The reaction mixture was stirred at 90 °C for overnight and upon completion, the solvent was evaporated under reduced pressure. The residue was diluted with ethyl acetate (20 mL) and the precipitate was filtered through Celite bed and washed with ethyl acetate (3 × 20 mL). The combined organic layer was washed with water and brine (3 × 20 mL) and dried over anhydrous sodium sulfate. The solvent was evaporated under reduced pressure to afford the crude product, which was purified by flash chromatography using 10% ethyl acetate in pet ether to afford the pure product **17** as white solid. $R_f = 0.5$ (10% ethyl acetate in pet ether). Yield: 0.11 g (38%); M.P. = 115–117 °C. ^{1}H-NMR ($CDCl_3$, 400 MHz): δ (ppm): 9.11 (dd, $J_1 = 8.5$ Hz, $J_2 = 1.0$ Hz, 1H), 8.60 (dd, $J_1 = 7.2$ Hz, $J_2 = 1.0$ Hz, 1H), 8.56 (d, $J = 7.3$ Hz, 1H), 8.29 (d, $J = 7.3$ Hz, 1H), 7.78 (dd, $J_1 = 8.4$ Hz, $J_2 = 7.3$ Hz, , 1H), 4.21-4.15 (m, 2H), 1.78-1.68 (m, 2H), 1.52-1.39 (m, 2H), 1.45 (s, 12H), 0.98 (t, $J = 7.4$ Hz, 3H). ^{13}C NMR (100 MHz, $CDCl_3$) δ (ppm): 164.4, 164.4, 135.8, 135.3, 134.9, 130.8, 129.7, 127.8, 127.0, 124.8, 122.6, 84.6, 40.3, 30.2, 25.0, 20.4, 13.9. ESI-MS (+ve) *m/z* calcd for $C_{22}H_{26}BNO_4$ $[M+H]^+$: 380.2030; found: 380.2030.

Synthesis of compound 6 [19]: To a mixture of compound **23** (30 mg, 0.11 mmol) and compound **31** (40 mg, 0.13 mmol) in anhydrous acetonitrile (2 mL) was added anhydrous K_2CO_3 (23 mg, 0.17 mmol) under argon atmosphere at 0 °C. After 30 min, the reaction mixture was allowed to attain room temperature and stirred for overnight. Upon completion of the reaction, solvent was evaporated under reduced pressure and the residue was diluted with ethyl acetate (50 mL). The mixture was washed with water and brine and the organic layer was dried over anhydrous sodium sulfate and evaporated under reduced pressure. The crude residue was purified by flash chromatography using 20% ethyl acetate in pet ether to afford the pure product **6** as bright green solid. $R_f = 0.5$ (20% ethyl acetate in pet ether); Yield: 60 mg (55%); M.P. = 166–168 °C. ^{1}H-NMR ($CDCl_3$, 600 MHz): δ (ppm): 8.61 (m, 2H), 8.52 (dd, $J_1 = 8.2$ Hz, $J_2 = 1.5$ Hz, 1H), 7.89 (d, $J = 7.9$ Hz, 2H), 7.71 (m, 1H), 7.52 (d, $J = 7.8$ Hz, 2H), 7.09 (dd, $J_1 = 8.3$ Hz, $J_2 = 1.0$ Hz, 1H), 5.39 (s, 2H), 4.17 (m, 2H), 1.71 (m, 2H), 1.45 (m, 2H), 1.36 (s, 12H), 0.97 (t, $J = 7.4$ Hz, 3H). ^{13}C NMR (150 MHz, $CDCl_3$) δ (ppm): 164.5, 164.0, 159.7, 138.5, 135.3, 133.3, 131.6, 129.4, 128.7, 126.7, 126.0, 123.6, 122.5, 115.4, 106.5, 84.0, 70.8, 40.1, 30.3, 24.9, 20.4, 13.9. ESI-MS (+ve) *m/z* calcd for $C_{29}H_{32}BNO_5$ $[M+H]^+$: 486.2452; found: 486.2483.

Synthesis of compound 18: To a stirred solution of triphosgene (0.13 g, 0.42 mmol) in anhydrous DCM (2 mL) was added pyridine (0.07 ml, 0.85 mmol) dropwise at ice-cold condition under argon atmosphere. The reaction mixture was stirred at room temperature for 30 min, then kept at −70 °C. To this solution, the compound **30** (0.20 g, 0.85 mmol) in dry DCM (2 mL) was added dropwise at that condition. Progress of the reaction was monitored by TLC analysis. Upon consumption of compound **30** completely, the mixture was added dropwise into the solution of compound **23** (0.11 g, 0.42 mmol) and triethylamine (0.06 mL, 0.42 mmol) in anhydrous DCM (5 mL) at −70 °C. Slowly the reaction mixture was warmed to room temperature and kept stirring for 2–3 h. Progress of the reaction was monitored by TLC analysis. Upon completion of the reaction, the excess triphosgene was quenched with water, extracted by DCM (3 × 20 mL). The combined organic layer was washed with brine (2 × 10 mL) and dried over anhydrous sodium sulfate. The solvent was evaporated under reduced pressure to afford the crude residue, which was purified by flash chromatography using 15% ethyl acetate in pet ether to afford the pure product **18** as white solid. $R_f = 0.5$ (20% ethyl acetate in pet ether). Yield: 60 mg (32%); M.P. = 131–132 °C. ^{1}H-NMR ($CDCl_3$, 400 MHz): δ (ppm): 8.62 (m, 2H), 8.32 (dd, $J_1 = 8.4$ Hz, $J_2 = 1.0$ Hz, 1H), 7.87 (d, $J = 8.0$ Hz, 2H), 7.77 (dd, $J_1 = 8$ Hz, $J_2 = 7.4$ Hz, 1H), 7.67 (d, $J = 8.1$ Hz, 1H), 7.47 (d, $J = 8.0$ Hz, 2H), 5.37 (s, 2H), 4.18 (t, $J = 8.0$ Hz, 2H), 1.70 (m, 2H), 1.45 (m, 2H), 1.36 (s, 12H), 0.98 (t, $J = 7.4$ Hz, 3H). ^{13}C NMR (150 MHz, $CDCl_3$) δ (ppm): 164.0, 163.4, 152.6, 151.4, 137.1, 135.2, 131.8, 131.7, 129.3, 127.7, 127.6, 127.4, 124.8, 122.9, 120.6, 118.6, 84.0, 71.0, 40.3, 30.2, 24.9, 20.4, 13.9. ESI-MS (+ve) *m/z* calcd for $C_{30}H_{32}BNO_7$ $[M + H]^+$: 530.2350; found: 530.2360.

Synthesis of compound 19 [33]: To a solution of bis(pinacolato) diboron (0.53 g, 2.09 mmol), compound **35** (0.50 g, 1.04 mmol), and KOAc (0.20 g, 3.12 mmol) in anhydrous 1, 4-dioxane (20 mL) was added $Pd(dppf)Cl_2$ (70 mg, 0.10 mmol) under argon atmosphere at room

temperature. The reaction mixture was stirred at 90 °C for 12 h. Upon completion, the solvent was evaporated under reduced pressure and the residue was diluted with ethyl acetate (20 mL). The mixture was filtered through Celite pad and washed with ethyl acetate (3 × 20 mL). The combined organic layer was washed with water and brine (3 × 20 mL) and the organic layer was dried over anhydrous sodium sulfate. The solvent was evaporated under reduced pressure to afford the crude product, which was purified by flash chromatography using 17% ethyl acetate in pet ether to afford the pure product **19** as white solid. $R_f = 0.5$ (20% ethyl acetate in pet ether); Yield: 0.38 g (58%); M.P. = 166–168 °C. ^{1}H-NMR ($CDCl_3$, 600 MHz): δ (ppm): 8.03 (d, $J = 7.4$ Hz, 1H), 7.74(s, 1H), 7.63 (m, 2H), 7.43 (dd, $J_1 = 7.8$ Hz, $J_2 = 0.7$ Hz, 1H), 7.12 (d, $J = 7.5$ Hz, 1H), 6.81 (d, $J = 7.8$ Hz, 1H), 6.77 (d, $J = 2.5$ Hz, 1H), 6.72 (d, $J = 8.8$ Hz, 1H), 6.62 (dd, $J_1 = 8.8$ Hz, $J_2 = 2.5$ Hz, 1H), 3.84 (s, 3H), 1.35 (s, 12H). ^{13}C NMR (150 MHz, $CDCl_3$) δ (ppm): 169.5, 161.4, 153.5, 152.4, 150.7, 135.1, 129.7, 129.4, 129.0, 127.2, 126.2, 125.1, 123.8, 123.5, 121.5, 111.7, 110.9100.9, 84.2, 82.7, 55.6, 24.9. ESI-MS (+ve) *m/z* calcd. for $C_{27}H_{25}BO_6$ $[M+H]^+$: 457.1822; found: 457.1841.

Synthesis of compound 20: The compound was prepared following the reported method with modifications [34]. To a stirred solution of compound **24** (0.20 g, 0.57 mmol) and compound **31** in anhydrous toluene (10 mL) was added silver oxide (0.20 g, 0.86 mmol) under inert atmosphere at room temperature. The reaction mixture was refluxed for 5 h. Progress of the reaction was monitored by TLC analysis. Upon completion, the solvent was evaporated under reduced pressure and the residue was diluted with dichloromethane (20 mL). The mixture was filtered through Celite pad and washed with DCM (3 × 10 mL). The combined organic layer was dried over sodium sulfate and the solvent was evaporated to afford the crude product. The crude product was purified by flash chromatography using 20% ethyl acetate in pet ether to afford the pure product **20** as yellow solid. $R_f = 0.5$ (20% ethyl acetate in pet ether) Yield: 0.12 g (37%); M.P. = 98–100 °C. ^{1}H-NMR ($CDCl_3$, 600 MHz): δ (ppm): 8.02 (d, $J = 7.6$ Hz, 1H), 7.83 (d, $J = 7.8$ Hz, 2H), 7.66 (t, $J = 7.2$ Hz, 1H), 7.61 (t, $J = 7.3$ Hz, 1H), 7.43 (d, $J = 7.7$ Hz, 2H), 7.15 (d, $J = 7.5$ Hz, 1H), 6.82 (s, 1H), 6.76 (d, $J = 2.2$ Hz, 1H), 6.68 (m, 3H), 6.60 (dd, $J_1 = 8.7$ Hz, $J_2 = 2.4$ Hz, 1H), 5.12 (s, 2H), 3.83 (s, 3H), 1.34 (s, 12H). ^{13}C NMR (150 MHz, $CDCl_3$) δ (ppm): 169.4, 161.3, 160.3, 153.2, 152.5, 152.4, 139.4, 135.1, 135.0, 129.7, 129.2, 129.1, 126.5, 126.5, 125.0, 124.0, 112.3, 111.7, 111.5, 111.2, 101.9, 100.8, 83.9, 83.2, 70.1, 55.6, 24.9. ESI-MS (+ve) *m/z* calcd for $C_{34}H_{31}BO_7$ $[M + H]^+$: 563.2241; found: 563.2275.

Synthesis of compound 21: To a stirred solution of compound **24** (0.20 g, 0.34 mmol) and triethylamine (0.14 mL, 1.04 mmol) in anhydrous DCM (8 mL) at 0 °C under argon atmosphere was dropwise added a solution of compound **32** (0.35 g, 0.86 mmol) in anhydrous DCM (2 mL). The mixture was then allowed to attain room temperature and stirred for 48 h. Progress of the reaction was monitored by TLC analysis. Upon completion, the reaction mixture was diluted with DCM (50 mL) and washed with water followed by saturated $NaHCO_3$ solution. The organic layer was washed with brine (3 × 10 mL) and dried over sodium sulfate. The solvent was evaporated under reduced pressure to afford the crude residue, which was purified by flash chromatography using 30% ethyl acetate in pet ether to afford the pure product **21** as off-white solid. $R_f = 0.5$ (30% ethyl acetate in pet ether). Yield: 80 mg (23%); M.P. = 100–102 °C. ^{1}H-NMR ($CDCl_3$, 600 MHz): δ (ppm): 8.03 (d, $J = 7.6$ Hz, 1H), 7.84 (d, $J = 7.9$ Hz, 2H), 7.68 (t, $J = 7.1$ Hz, 1H), 7.63 (t, $J = 7.3$ Hz, 1H), 7.44 (d, $J = 7.9$ Hz, 2H), 7.16 (m, 2H), 6.88 (dd, $J_1 = 8.7$ Hz, $J_2 = 2.3$ Hz, 1H), 6.81 (d, $J = 8.7$ Hz, 1H), 6.78 (d, $J = 2.4$ Hz, 1H), 6.70 (d, $J = 8.8$ Hz, 1H), 6.63 (dd, $J_1 = 8.8$ Hz, $J_2 = 2.5$ Hz, 1H), 5.29 (s, 2H), 3.84 (s, 3H), 1.35 (s, 12H). ^{13}C NMR (150 MHz, $CDCl_3$) δ (ppm): 169.3, 161.5, 153.0, 152.2, 152.1, 151.8, 137.4, 135.2, 135.1, 129.9, 129.2, 129.0, 127.6, 126.4, 125.1, 124.0, 117.0, 116.9, 112.0, 110.8, 109.8, 100.8, 84.0, 82.4, 75.0, 70.5, 55.6, 24.9. ESI-MS (+ve) *m/z* calcd for $C_{35}H_{31}BO_9$ $[M+H]^+$: 607.2139; found: 607.2187.

2.3. UV–visible and fluorescence spectroscopic studies

All the stock solution of probes and the released fluorophores were prepared in spectroscopy grade DMSO (note: 20% THF was added with DMSO for the naphthalimide-based probes **17**, **6** and **18** to dissolve them completely) and the stock solution of hydrogen peroxide was prepared freshly in mili-Q water. All the spectroscopic studies were performed under physiological conditions (phosphate buffer, 20 mM, pH = 7.5). Buffers with higher pH (8, 9 and 10) were prepared by adding 1 N NaOH solution to the buffer. Samples for absorption and emission spectroscopic measurements were carried out in quartz cuvettes (1.0 ml). UV–Vis spectroscopic analyses were performed on a Lambda 45 UV–Vis spectrophotometer and fluorescence emission spectra were recorded on a Fluoromax-4 spectrophotometer (FluoroMax-4, HORIBA). For coumarin-based probes, $\lambda_{ex} = 322$ nm and $\lambda_{em} = 447$ nm with slit width = 3/3 nm, for naphthalimide-based probes, $\lambda_{ex} = 442$ nm and $\lambda_{em} = 550$ nm with slit width = 5/5 nm and for fluorescein-based probes, $\lambda_{ex} = 454$ nm and $\lambda_{em} = 511$ nm with slit width = 3/3 nm were used in the fluorescence emission spectroscopic studies. The selectivity of the directly-linked probe **19** (10 μM) towards H_2O_2 (200 μM) was carried out over different analytes such as *tert*-butyl hydroperoxide (*t*Bu-OOH), cumene hydroperoxide (Cum-OOH), potassium superoxide (KO_2, O_2^-), reduced glutathione (GSH), L-cysteine (CYS), *N*-acetyl cysteine (NAC), sodium chloride (NaCl) and potassium chloride (KCl). The probe was initially incubated with the analytes (200 μM) for 30 min and the emission intensity was measured. An equal amount of H_2O_2 (200 μM) was added to the resulting solution and the emission was measured after incubation of another 30 min.

2.4. Determination of limit of detection (LOD) of the probes

The limit of detection (LOD) of all the fluorescein-based probes **19**, **20** and **21** were determined using the fluorescence titration. The detection limit was calculated using the equation, LOD = 3σ/K, where σ is the standard deviation of blank measurements (without H_2O_2) and K is the slope of emission intensity versus H_2O_2 concentration. To get the standard deviation of the blank measurements, the emission intensity of all the probes (10 μM) were measured 10 times in the absence of H_2O_2. For the determination of slopes, the emission spectra were measured at different concentrations of H_2O_2 (2–50 μM) after incubating each reaction mixture for 30 min.

2.5. Analysis of reaction kinetics using reverse phase HPLC method

Purity of the synthesized compounds were analyzed by analytical high performance liquid chromatography (HPLC), Agilent 1220 infinity II LC system using reverse phase C_{18} column (Luna®, 250 × 4.6 mm, 5 μm). HPLC Chromatogram of the compounds **19**, **20** and **21** were detected by PDA detector at 254 nm and 454 nm at room temperature using a flow rate of 1.0 ml/min over 15 min. Concentrations of the pure probes and the released fluorophores were 100 μM and in the reaction mixture, 100 equivalents of H_2O_2 (10 mM) was added. The reactions of probes with H_2O_2 were carried out in HPLC grade acetonitrile and water system (3:1) at room temperature and the samples were injected into the system at different time intervals to monitor the progress of the reaction.

2.6. Detection of endogenous level of H_2O_2 in HeLa cells by cellular imaging

HeLa cells were cultured in high glucose Dulbecco's modified Eagle's medium (DMEM) supplemented with 10% fetal bovine serum (FBS) and 1% penicillin/streptomycin at 37 °C under 5% CO_2 atmosphere. Cells were then plated (0.5×10^4 cells/plate) in 35 mm cell culture petri dishes containing 2.0 mL of DMEM and incubated at 37 °C under 5% CO_2 for 24 h. The confluent cells were washed with DPBS and finally incubated with the fluorescein-based probes (**19**–**21**) (5.0 μM) at 37 °C

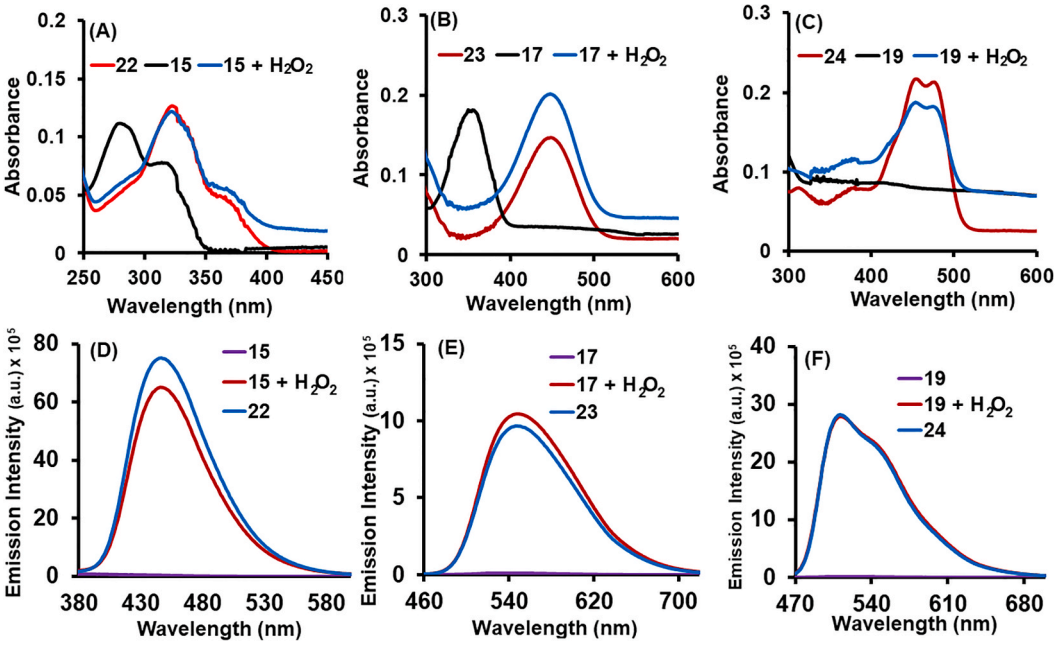

Fig. 1. Absorption (A–C) and emission (D–F) spectra of directly-linked probes **15**, **17** and **19** (10 μM) in the absence and presence of H_2O_2 (200 μM) along with the spectra of pure released fluorophores (**22**–**24**, 10 μM) in phosphate buffer of pH 7.5. The final spectra of the probes with H_2O_2 were recorded after 90 min.

under 5% CO_2 for 1 h. After washing with DPBS (5 times), cellular morphology was carefully observed and imaged in a Bio-Rad ZOE™ fluorescent cell imager under bright field and suitable fluorescent colored filters. Additionally, the control experiments were designed and performed with the pre-treatment of NAC (*N*-acetyl cysteine) (2.0 mM) to the HeLa cells to affirm the quenching of endogenous ROS or hydrogen peroxide level. The cells were washed with DPBS and treated further with the fluorogenic probes and incubated for 1 h. Finally, the treated cells were washed with DPBS (5 times) and imaged in a Bio-Rad ZOE™ fluorescent cell imager to understand the reactivity of hydrogen peroxide with fluorescent probes. Further, to confirm the sensitivity of the boronate ester-based probes towards hydrogen peroxide, exogenous H_2O_2 (200 μM) was added to the cells and incubated at 37 °C under 5% CO_2 for 1 h. The cells were washed with DPBS and probes (**19**–**21**) (5.0 μM) were added and incubated as discussed above. Finally, after sequential washing with DPBS, treated cells were imaged under Bio-Rad ZOE™ fluorescent cell imager.

2.7. Cell culture and cellular viability studies

Human cervical cancer cell line (HeLa) was obtained from the National Centre for Cell Science (NCCS), Pune, India. HeLa cells were cultured in DMEM medium (Gibco) supplemented with 10% (v/v) FBS (Gibco) and 1% Pen-Strep (Gibco). Cells were cultured as a monolayer in a humidified incubator at 37 °C in the presence of 5% CO_2 level. All the coumarin-based, naphthalimide-based and fluorescein-based turn-on fluorescent probes along with the corresponding released fluorophores (**22**–**24**) were screened for their anti-proliferative activities using the conventional MTT assay. All the test compounds were dissolved in DMSO (HiMedia) except naphthalimide-based probes (stock solution was prepared in THF and diluted further using media with final THF concentration kept below 0.05%). HeLa cells were seeded in 96-well culture plates at a density of 1×10^4 cells/100 μl/well and treated with the freshly prepared test compounds (5.0, 10.0 and 25.0 μM) for 0 h (control) and 48 h (experimental). At the end of treatment period, 10.0 μL of 5.0 mg/mL of MTT was added to the plate (control) and incubated for 4 h. Following the 4 h incubation, the culture media from the plate was removed and the purple formazan crystals were dissolved using 100 μL of DMSO (HiMedia) and the absorbance at 570 nm was measured using a microplate reader (Multiskan Go microplate reader, Thermo Scientific). In experimental set, similar MTT treatment protocol was followed only after 48 h. The mean ΔOD values were calculated by the subtraction of mean OD values of 0 h plate (control) from the mean OD values of identical wells at 48 h plate (experimental) and the percentage proliferation was calculated keeping the mean ΔOD of untreated control as 100%.

3. Results and discussion

3.1. Design and synthesis of the probes

In the present study, three different sets of turn-on fluorescent probes were developed considering fluorophores **22**–**24** (experimental section and Schemes S1–S4, supplementary information section). In the first set, boronic ester group was incorporated directly to the aromatic nuclei with the replacement of hydroxyl group (probes **15**, **17** and **19**). The boronic ester group was installed by the Pd-catalyzed transmetalation reaction of triflate/bromide derivative of the fluorophores with bis (pinacolato)diboron under inert conditions. In the second set, the boronate benzyl alcohol moiety was installed on the fluorophores *via* ether linkage (probes **16**, **6** and **20**). These probes were synthesized by the coupling of fluorophore alcohols with boronate benzyl bromide in the presence of Cs_2CO_3 or K_2CO_3. Whereas, in the third set, the boronate benzyl alcohol was coupled to the fluorophores *via* carbonate linkage (probes **12**, **18** and **21**). These probes were achieved either by the coupling of fluorophore alcohols with 4-nitrophenyl carbonate adduct of boronate benzyl alcohol or by the conventional coupling using triphosgene. All the final boronate ester-based probes, obtained in reasonably good yields, were purified and characterized by analytical methods before the planned spectroscopic studies.

3.2. Absorption and emission spectroscopic studies

The initial UV–Vis spectroscopic studies were carried out with the directly-linked probes (**15**, **17** and **19**) with and without H_2O_2 to identify the absorption maxima of the intact probes and the released fluorophores. As shown in Fig. 1 (A-C), a significant red-shift was observed upon their reactions with H_2O_2 and the spectra overlapped well with

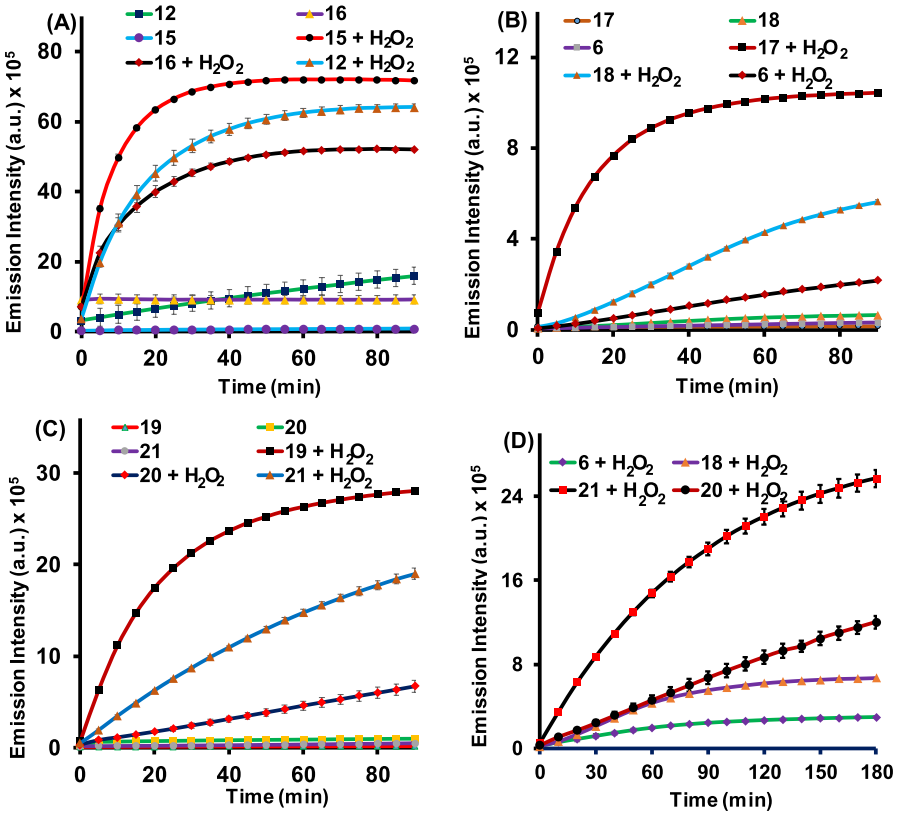

Fig. 2. Emission spectra of (A) coumarin-, (B) naphthalimide- and (C) fluorescein-based probes (10 μM) with and without H_2O_2 (200 μM) over 90 min in phosphate buffer (20 mM) of pH 7.5. (D) Emission spectra of self-immolative probes (**6**, **18**, **20** and **21**) (10 μM) in the presence of H_2O_2 (200 μM) over a longer time (180 min) under identical condition.

that of pure fluorophores (**22**–**24**). For the probe **19**, very weak absorption band above 300 nm was probably due to the protection of both hydroxyl groups in fluorescein. Knowing the absorption maxima of all fluorophores **22**–**24**, the turn-on fluorescence efficacy of the probes **15**, **17** and **19** were evaluated using fluorescence spectroscopy. As shown in Fig. 1 (D-F), highly intense emission response was observed for all the probes in the presence of H_2O_2 and the emission pattern matched well with that of the respective released fluorophores, indicating the H_2O_2-triggered turn-on fluorescence. The absorption and emission spectra of other probes with and without H_2O_2 are shown in the supplementary information (Figs. S1–S2, ESI).

3.3. Kinetic studies using fluorescence spectroscopy

With the preliminary results in hand, we carried out kinetic experiments to understand the relative reactivity of all the boronate ester linked probes in the presence of H_2O_2 up to 90–180 min. As shown in Fig. 2A, a clear difference in the relative reactivity/sensitivity among the coumarin-based probes (**15**, **16** and **12**) towards H_2O_2 is observed. A significantly higher reactivity is noted for the directly-linked probe **15** and the lowest reactivity was noted for the ether-linked probe **16**. While probe **15** was highly reactive towards H_2O_2 and the reaction was almost saturated within 30 min, the saturation time was found to be relatively longer for the corresponding self-immolative probes. Interestingly, a

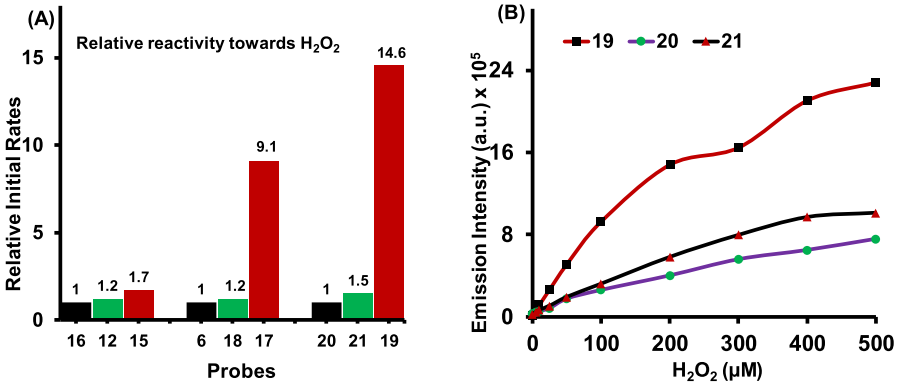

Fig. 3. (A) Relative initial rates for the turn-on fluorescence of carbonate-linked (green) and directly-linked (red) probes w.r.t ether-linked (black) probes of a particular fluorophore in their reactions with H_2O_2. (B) Emission spectra of fluorescein-based probes (**19**–**21**, 10 μM) in the presence of variable concentrations of H_2O_2 (0–500 μM) with a fixed incubation time of 30 min.

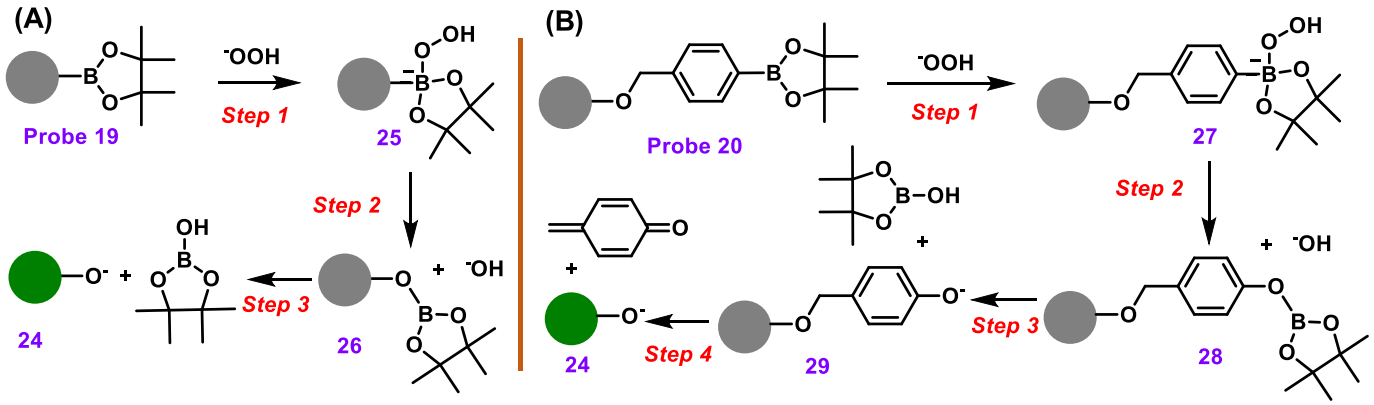

Scheme 2. Generalized and most plausible mechanistic pathways for the reactions of fluorescein-based directly-linked probe **19** (A) and ether-linked self-immolative probe **20** towards H_2O_2 for the release of fluorophore **24**.

similar but more pronounced effect is observed for naphthalimide- and fluorescein-containing probes. For example, the initial saturation time was much longer for the directly-linked probes **17** and **19** (~50 min) as compared to **15** (~30 min). This indicates the higher reactivity of coumarin-based directly-linked boronate ester probes than the corresponding naphthalimide- and fluorescein-based probes. Furthermore, the self-immolative probes corresponding to naphthalimide (**6** and **18**) and fluorescein (**20** and **21**) fluorophores were found to be much less reactive than the corresponding directly-linked probes **17** and **19** (Fig. 2B and C). Between, two types of self-immolative probes, the reactivity of the ether-linked probes were found to be lower than the carbonate-linked probes in general. Furthermore, it should be noted here that, like coumarin-based probes, typical saturation kinetics was not observed for naphthalimide- and fluorescein-based self-immolative probes till 90 min and therefore, the kinetic experiments were extended up to 180 min to understand their nature of kinetic pattern (Fig. 2D). Interestingly, while some level of saturation kinetics was observed with relatively higher emission intensity for the carbonate-linked probes (**18** and **21**), both the ether-linked probes (**6** and **20**) reflected lower and almost steep increasing intensity pattern without saturation up to 180 min (Fig. 2D). These results clearly indicate the higher reactivity of directly-linked boronate ester probes than the corresponding self-immolative linker-based probes.

3.4. Nature of fluorophore unit on probe efficiency

The fluorophore dependency of the relative rate of fluorescence turn-on from three types of boronate ester-linked probes was evidenced in Fig. 3. As shown in Fig. 3A, the difference in relative initial rate of reaction between two different kinds of self-immolative probes was not significant for all three fluorophores and in general, the carbonate-linked probes were slightly more reactive than the corresponding ether-linked probes. However, a significantly higher difference in relative rate is observed between the directly-linked probes and the ether-linked probes towards H_2O_2. Furthermore, this difference was found to be dependent on the nature of fluorophore unit being used. For example, the difference was 14.6-fold, 9.1-fold and 1.7-fold for fluorescein-, naphthalimide- and coumarin-based probes, respectively (Fig. 3A). The above difference in turn-on response of directly-linked and self-immolative-linked probes form various fluorophores appears to be inversely proportional to the reactivity of directly-linked probes of various fluorophores towards H_2O_2. For example, as the coumarin-based probes react much faster with H_2O_2 than the naphthalimide- and fluorescein-based probes, the difference in fluorescence response of directly-linked and self-immolative-linked probes is less pronounced for coumarin-based probes than two other fluorophore-based probes. Overall, the kinetic experiments clearly reveal the better suitability of directly-linked boronate ester probes for sensing traces of H_2O_2. However, the ether- or carbonate-based self-immolative probes might be suitable for H_2O_2-triggered drug delivery applications, often requiring sustained drug release profiles [23,35,36].

While both of naphthalimide and fluorescein fluorophores (**23** and **24**) have almost similar emission ranges (yellow color, naked eye), the turn-on fluorescence emission intensity from the fluorescein-based probes (**19**–**21**) were higher than that from the naphthalimide-based probes (**17**, **6** and **18**) under identical condition at a fixed concentration (10 μM) in the presence of H_2O_2 (200 μM). Furthermore, the solubility profiles of naphthalimide-based probes were much narrower than that of fluorescein-based probes. Naphthalimide-based probes were soluble only in THF and not completely soluble in other polar solvents such as DMSO, DMF, ACN and water. However, fluorescein-based probes were soluble in a wider ranges of polar organic solvents including the solvents mentioned above except water. Due to these reasons, fluorescein-based probes (**19**–**21**) were chosen for further studies. A significant difference in kinetic pattern of probes **19**–**21** (10 μM) with 200 μM H_2O_2 (20-fold) inspired us to understand their behavior with a varied concentration of peroxide (0–500 μM) at a fixed incubation time (30 min). Interestingly, as shown in Fig. 3B, a clear difference in emission intensity was observed at lower concentration and the difference increased gradually with H_2O_2 concentration, supporting our views that directly-linked probe **19** is much efficient in sensing H_2O_2 than probes **20** and **21**.

3.5. Sensitivity of the probes

To further understand the relative sensitivity of fluorescein-based probes **19**–**21** towards H_2O_2, the limit of detection (LOD) was calculated as per standard method using fluorescence titration [29]. The emission intensity of the probes (10 μM) was measured in the absence of H_2O_2 and at a lower variable concentration range (2–50 μM) of H_2O_2. Interestingly, a significant difference in the sensitivity of probes **19**–**21** towards H_2O_2 was observed. For example, while the LOD of directly-linked boronate ester probe **19** was 33 nM, the LOD of ether- and carbonate-linked probes (**20** and **21**) were significantly higher (1.3 and 0.37 μM, respectively), indicating much higher sensitivity of **19** than **20** and **21** (Fig. S3, Table S2, ESI). It should be noted here that the result on their relative sensitivity matches well with their fluorescence turn-on response over time and analyte concentration (Figs. 2C and 3B).

3.6. Mechanistic insights for turn-on fluorescence process

To understand possible reasons for the relatively slower reactivity of self-immolative probes over the directly-linked probes, the underlying stepwise mechanistic pathways were proposed depicting the reaction of

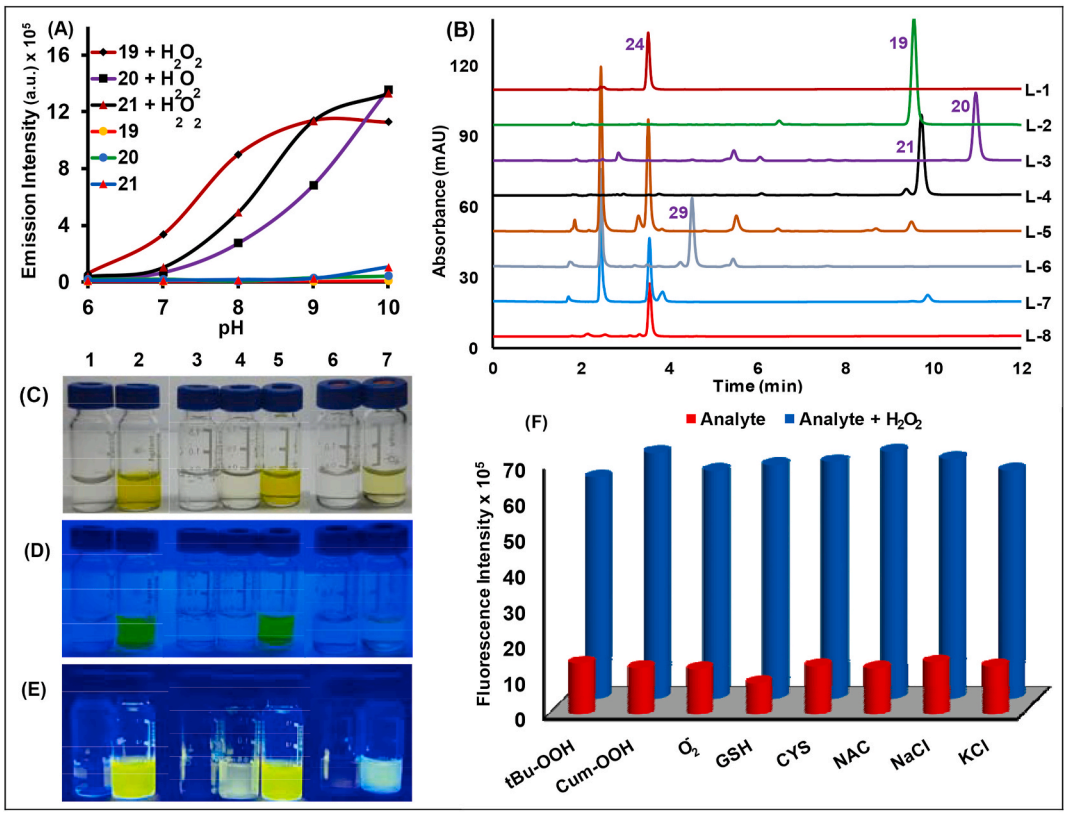

Fig. 4. (A) Emission spectra of probes **19**–**21** (3 μM) in the absence and presence of H_2O_2 (200 μM) at variable pH of the medium. (B) HPLC chromatogram of pure probes **19**–**21**, released fluorophore (**24**) and the reaction mixtures of probes (100 μM) + H_2O_2 (10 mM) after 30 min. L-1: pure **24**; L-2 to L-4: pure probes **19**–**21**; L-5: **19** + H_2O_2; L-6: **20** + H_2O_2; L-7: **21** + H_2O_2; L-8: **20** + H_2O_2 + NaOH (25 mM). The chromatograms L-1 to L-7 were visualized at 254 nm and L-8 was visualized at 454 nm to monitor the released fluorophore **24**. Peak at 2.46 min appears from the stabilizers in commercial H_2O_2 sample. (C) Vials under visible light; (D) under UV light (254 nm); (E) under fluorescent light (366 nm); Pure probes **19**–**21** (vials 1, 3 and 6); probes **19**–**21** + H_2O_2 (vials 2, 4 and 7); probe **20** + H_2O_2 + NaOH (vial 5). (F) Reactivity of the directly-linked probe **19** (10 μM) towards different analytes (200 μM) followed by the treatment with H_2O_2 (200 μM). The probe was initially incubated with the analytes for 30 min and the emission intensity was measured. Final response was measured upon the addition of H_2O_2 (200 μM) to the resulting solution followed by the incubation for another 30 min.

representative fluorescein-based probes **19** and **20** towards H_2O_2 (Scheme 2). The plausible reaction pathways for the reaction of boronate ester group with H_2O_2 is well-established and is used extensively in turn-on fluorescence processes [37,38]. The initial nucleophilic reaction of hydroperoxide anion at the electrophilic boron-center of the directly-linked probe **19** followed by the rearrangement and subsequent nucleophilic attack of hydroxyl anion leads to the release of fluorescein fluorophore **24** with turn-on fluorescence (Scheme 2A). However, a similar process in probe **20** would generate the intermediate **29**. From Scheme 2B, it is evident that, unlike probe **19**, the fluorescence will be turned-on from **20** only after the self-immolation of benzyl group in the intermediate **29** *via* quinone methide (QM) species, generation of which is quite well-established for the self-immolative fluorogenic probes (Step 4, Scheme 2B) [18,25].

3.7. pH responsiveness of the probes

To understand the feasibility of turn-on fluorogenic process and the stability of the probes over a wider range of pH, the emission studies were carried out with variable pH (6.0–10.0) of the medium. Interestingly, a steady increased emission pattern was observed for the probe **19** with increasing pH of the medium from 6 to 8 and the emission almost saturates at pH 9. In contrast, steep increase in emission intensity was observed for both the self-immolative probes **20** and **21** with increasing pH of the medium and eventually that crossed the emission intensity from the probe **19** (Fig. 4A). This is not surprising as increasing pH would facilitate the reaction by partial conversion of H_2O_2 to hydroperoxide ion (HOO^-; *p*Ka of H_2O_2: 11.6). Furthermore, the self-immolation process *via* QM intermediate would also be enhanced by the predominant existence of phenoxide ion in the intermediate **29** (Scheme 2B) at higher pH ranges (*p*Ka of phenols: ~10). Additionally, the experiment further evidenced the overall stability of probes **19**–**21** in the absence of H_2O_2 over a wide pH range of the medium indicating their compatibility under normal physiological as well as pathological conditions.

3.8. Kinetic studies using reverse phase HPLC method

The relative reactivity of the boronate ester groups in probes **19**–**21** towards H_2O_2 was studied by kinetic experiments using reverse phase HPLC method (Fig. 4B). Interestingly, while a clean conversion of the directly-linked probe **19** to the fluorophore **24** was observed in the presence of H_2O_2 with time (L-5, Fig. 4B), the self-immolative probe **20** produced the intermediate phenolic compound **29**, which was quite persistent under HPLC condition in acetonitrile and water (3:1) mixture with traces of fluorophore (**24**) release (L-6, Fig. 4B). However, the intermediate **29** could be rapidly converted to fluorophore **24** upon the treatment of NaOH solution (L-8). The formation of **29** was also evidenced in ESI-MS analysis (Fig. S8, ESI). The carbonate-linked probe **21** rather reacted rapidly with the release of fluorophore **24** and probably with very traces of intermediate (L-7, Fig. 4B, Fig. S6, ESI). The peak at around 2.46 min with almost fixed intensity appears from the sample of commercially available H_2O_2 (Merck, India), which is probably originated from the stabilizers used in H_2O_2. The relative formation of

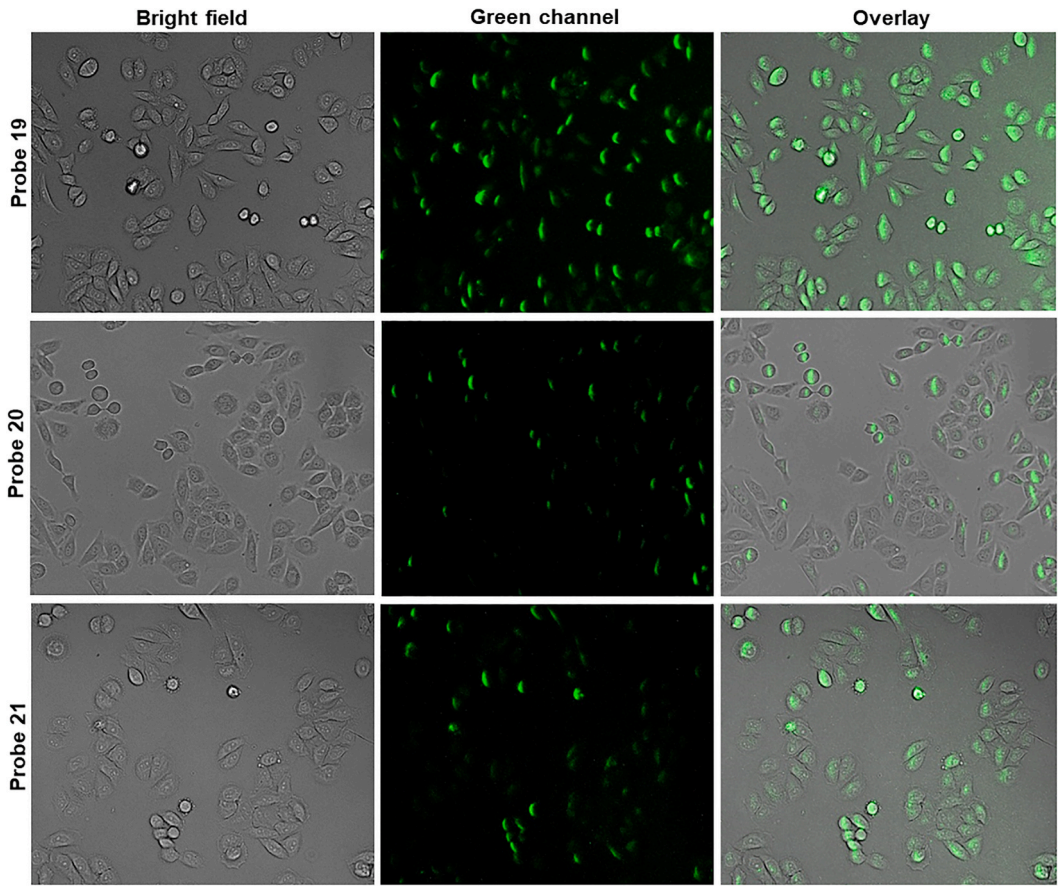

Fig. 5. Fluorescence microscopy images (bright field, green channel and overlay) of HeLa cells in the presence of fluorescein-based probes **19**–**21** for the detection of endogenous level of H_2O_2.

released fluorophore **24** from probes **19**–**21** in the presence of H_2O_2 over 60 min was also estimated and the results show significantly higher release of **24** from the directly-linked probe **19** over other two self-immolative linker-based probes **20**–**21** (Fig. S7, ESI).

The difference in fluorescence turn-on process for the fluorescein-based probes **19**–**21** can be clearly visualized with naked eyes (Fig. 4C) and also upon irradiation with UV (Fig. 4D) and fluorescence light (Fig. 4E). These observations indicate that the boronate ester cleavage process by H_2O_2 is reasonably fast for all the probes and the difference in fluorescence emission response from the directly-linked and self-immolative linker-based probes is mainly due to the relatively slower rate of self-immolative processes *via* QM intermediate particularly for the ether-linked probes. Our observation with significantly higher fluorescence-response for the directly linked boronate ester probes than self-immolative probes is found to be in contrast to the behavior and reactivity of non-fluorogenic peroxide-sensitive methyl salicylate-based inhibitors of metalloproteinase and the 2,4-dinitrophenyl group-based NIR probes for thiophenol sensing [39,40].

3.9. Selectivity of the directly-linked probe *19* towards H_2O_2

Considering the evidences that directly-linked probe **19** exhibited significantly higher reactivity towards H_2O_2 than that of the corresponding self-immolative probes **20** and **21**, the selectivity of the probe towards H_2O_2 was studied. Some of the oxidizing agents, reducing agents and inorganic salts were chosen to see their relative impacts on the selectivity of probe **19** towards H_2O_2. The probe (10 μM) was first incubated with various analytes (200 μM) and the emission intensity was measured (red cylinders, Fig. 4F). To the solution mixture, H_2O_2 (200 μM) was added and the final emission was measured (blue cylinders, Fig. 4F) following the similar protocol. As shown in Fig. 4F, a significant enhancement of the emission intensity was observed upon the addition of H_2O_2 in the presence of all the analytes studied herein. We like to mention here that the directly-linked probe was reported by Chang and co-workers in 2010 along with few other directly-linked probes and showed the enhanced selectivity of the probes towards H_2O_2 over other relevant oxidants and radicals [33].

3.10. Detection of the endogenous level of H_2O_2 in HeLa cells

To understand the compatibility of the probes in cellular medium for the detection of endogenous level of H_2O_2, the probes (5.0 μM) were treated to human cervical cancer cells (HeLa) and the emission was measured after 60 min (Fig. 5). Interestingly, a significantly higher emission response under green channel was observed for the probe **19** as compared to **20** and **21**. The emission response was much weaker for the ether-linked probe **20** under the identical condition, indicating much lesser sensitivity of **20** in detecting the endogenous level of H_2O_2 in HeLa cells. To understand the selectivity of the directly-linked probe **19** towards the endogenous level of H_2O_2, HeLa cells were pre-treated with *N*-acetyl cysteine (NAC, 2.0 mM) that scavenges the endogenous H_2O_2. Interestingly, no emissive response in the NAC pre-treated cells served as the negative control and also evidenced the lack of any background emission response of the probe **19** (Fig. S10, ESI). This also proved the stability of probe **19** under cellular environment. Positive control experiments were also carried out upon the exogenous addition of H_2O_2 to the cells followed by the treatment of probe **19**. Interestingly, enhanced intensity from all the probes upon exogenous treatment of H_2O_2 to the cells further confirms the peroxide-responsive fluorescence turn-on process (Fig. S11, ESI) under cellular environment and the suitability

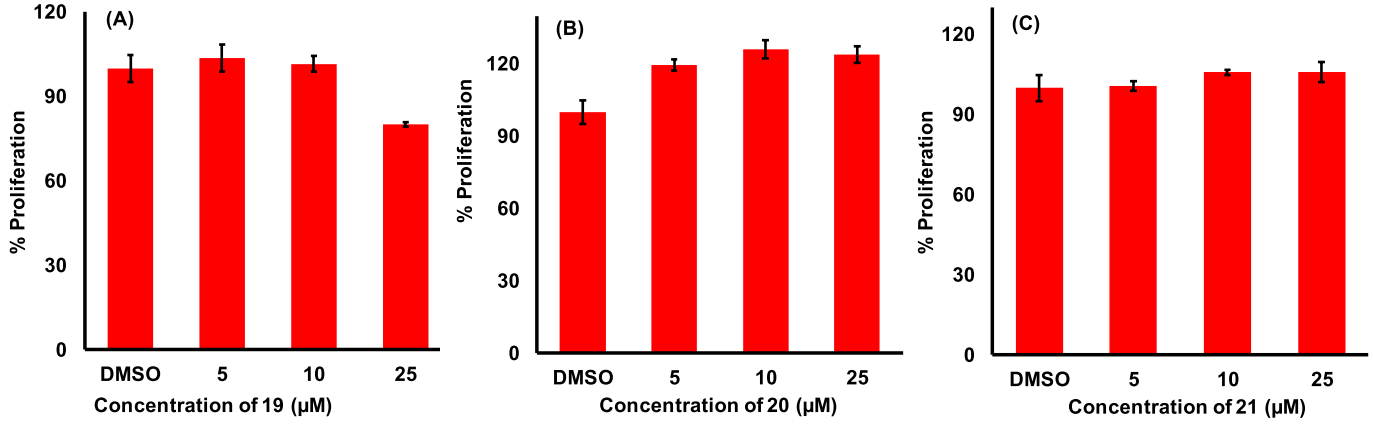

Fig. 6. Cellular viability of HeLa cells in the presence of probes **19**–**21** at variable doses (5.0, 10.0 and 25.0 μM). The cells were incubated with the probes for 48 h at 37 °C in humidified incubator in the presence of 5% CO_2 level.

of these probes for sensing the endogenous level of H_2O_2. Emission response of the naphthalimide-based probes were also studied for the detection of endogenous level of H_2O_2 in HeLa cells under identical condition, however, the images had background noises (Fig. S9, ESI).

3.11. *Toxicity profiles of the probes*

To understand the compatibility of the turn-on fluorogenic probes in cellular medium, their toxicity profiles were studied in the same cell line (HeLa) using conventional MTT assay. While imaging studies were carried out with 5.0 μM of the probes, toxicity profiles of the probes were evaluated at 5.0 μM and at two higher concentration levels (10.0 and 25.0 μM) and incubated for a longer time (48 h). Interestingly, all the probes were found to be non-toxic at 5.0 and 10.0 μM concentrations indicating the feasibility of their applications in cellular medium (Fig. 6 and Fig. S12, ESI). However, few of them exhibited around 20% cellular toxicity at a 5-fold higher concentration (25.0 μM). Although, the directly-linked boronate ester probes were found to be significantly more sensitive than the self-immolative linker-based probes of naphthalimide and fluorescein fluorophores for sensing H_2O_2 , further analysis might be necessary considering a wider ranges of fluorophore units for a more generalized understanding.

4. Conclusions

In summary, we highlight for the first time that direct coupling of the boronate ester group to the fluorophore unit in peroxide-responsive turn-on fluorogenic probes is strategically superior than the coupling *via* self-immolative linkers in effectively sensing traces of H_2O_2 both in aqueous and cellular medium. Moreover, the turn-on efficiency is also dependent on the nature of fluorophore units used. Considering both and based on several control experiments, fluorescein-based directly-linked probe **19** was found to be the best candidate among all the probes studied in the present report for its application in sensing H_2O_2 accurately. While directly coupled boronate ester probes are shown to be suitable for sensing peroxide effectively, the self-immolative linker-based probes may find wider applications in peroxide-triggered drug delivery systems that require a slower, sustained and regulated drug release profile. Despite the availability of many boronate ester-based probes, outcome of this study would certainly be useful as a guideline while designing a new boronate ester-based probe for sensing peroxide or utilizing them particularly in ROS-associated pathologies and therapies in future.

CRediT authorship contribution statement

Abu Sufian: optimized the experimental condition. **Debojit Bhattacherjee:** carried out cellular experiments and fluorescent microscopic experiments. **Tripti Mishra:** compounds and intermediates and characterized the products. **Krishna P. Bhabak:** Supervision, Formal analysis.

Declaration of competing interest

The authors declare that they have no known competing financial interests or personal relationships that could have appeared to influence the work reported in this paper.

Acknowledgements

K.P.B. acknowledges SERB for the research grant (Ref: EEQ/2016/000090). K.P.B. thanks DST, India for the INSPIRE Faculty Award. We acknowledge DST-FIST program, CoE-FAST and IIT Guwahati for infrastructural facilities. A.S. and D.B. thank IIT Guwahati for their fellowships.

Appendix A. Supplementary data

Supplementary data to this article can be found online at https://doi.org/10.1016/j.dyepig.2021.109363.

References

[1] Sies H. Redox Biol 2017;11:613–9.
[2] Ohshima H, Tatemichi M, Sawa T. Arch Biochem Biophys 2003;417:3–11.
[3] Shah AM, Channon KM. Heart 2004;90:486–7.
[4] Sies H. Am J Med 1991;91:S31–8.
[5] Barnham KJ, Masters CL, Bush AI. Nat Rev Drug Discov 2004;3:205–14.
[6] Bhabak KP, Mugesh G. Acc Chem Res 2010;43:1408–19.
[7] Liang J, Liu B. Bioeng Translational Medicine 2016;1:239–51.
[8] Chen X, Wang F, Hyun JY, Wei T, Qiang J, Ren X, Shin I, Yoon J. Chem Soc Rev 2016;45:2976–3016.
[9] Wang R, Bian Z, Zhan D, Wu Z, Yao Q, Zhang G. Dyes Pigments 2021;185:108885.
[10] Lippert AR, Van de Bittner GC, Chang CJ. Acc Chem Res 2011;44:793–804.
[11] Galbraith E, James TD. Chem Soc Rev 2010;39:3831–42.
[12] Wu L, Sedgwick AC, Sun X, Bull SD, He X-P, James TD. Acc Chem Res 2019;52:2582–97.
[13] Lo L-C, Chu C-Y. Chem Commun 2003:2728–9.
[14] Chang MCY, Pralle A, Isacoff EY, Chang CJ. J Am Chem Soc 2004;126:15392–3.
[15] Albers AE, Okreglak VS, Chang CJ. J Am Chem Soc 2006;128:9640–1.
[16] Kim E-J, Bhuniya S, Lee H, Kim HM, Cheong C, Maiti S, Hong KS, Kim JS. J Am Chem Soc 2014;136:13888–94.
[17] Liang X, Xu X, Qiao D, Yin Z, Shang L. Chem Asian J 2017;12:3187–94.
[18] Daniel KB, Agrawal A, Manchester M, Cohen SM. Chembiochem 2013;14:593–8.
[19] Liu C, Shao C, Wu H, Guo B, Zhu B, Zhang X. RSC Adv 2014;4:16055–61.

[20] Yi L, Wei L, Wang R, Zhang C, Zhang J, Tan T, Xi Z. Chem Eur J 2015;21:15167–72.
[21] Zhang Y-J, Wang X, Zhou Y, Zhao K, Wang C-K. Chem Phys Lett 2016;662:107–13.
[22] Li W, Wang X, Zhang Y-M, Zhang SX-A. Dyes Pigments 2018;148:348–52.
[23] Zhu J, Chen J, Song D, Zhang W, Guo J, Cai G, Ren Y, Wan C, Kong L, Yu W. J Mater Chem B 2019;7:7548–57.
[24] Srikun D, Miller EW, Domaille DW, Chang CJ. J Am Chem Soc 2008;130:4596–7.
[25] Chung C, Srikun D, Lim CS, Chang CJ, Cho BR. Chem Commun 2011;47:9618–20.
[26] Kim D, Kim G, Nam S-J, Yin J, Yoon J. Sci Rep 2015;5:8488.
[27] Hanna RD, Naro Y, Deiters A, Floreancig PE. J Am Chem Soc 2016;138:13353–60.
[28] Xiao H, Li P, Hu X, Shi X, Zhang W, Tang B. Chem Sci 2016;7:6153–9.
[29] Xu J, Zhang Y, Yu H, Gao X, Shao S. Anal Chem 2016;88:1455–61.
[30] Liu T, Zhang X, Qiao Q, Zou C, Feng L, Cui J, Xu Z. Dyes Pigments 2013;99:537–42.
[31] Zhang J, Sun Y-Q, Liu J, Shi Y, Guo W. Chem Commun 2013;49:11305–7.
[32] Mukhopadhyay A, Maka VK, Moorthy JN. Phys Chem Chem Phys 2017;19:4758–67.
[33] Dickinson BC, Huynh C, Chang CJ. J Am Chem Soc 2010;132:5906–15.
[34] More KN, Lim T-H, Kim S-Y, Kang J, Inn K-S, Chang D-J. Dyes Pigments 2018;151:245–53.
[35] Saravanakumar G, Kim J, Kim WJ. Adv Sci 2017;4:1600124.
[36] Wang X, Li X, Liang X, Liang J, Zhang C, Yang J, Wang C, Kong D, Sun H. J Mater Chem B 2018;6:1000–10.
[37] Purdey MS, McLennan HJ, Sutton-McDowall ML, Drumm DW, Zhang X, Capon PK, Heng S, Thompson JG, Abell AD. Sensor Actuator B Chem 2018;262:750–7.
[38] Mori S, Morihiro K, Okuda T, Kasahara Y, Obika S. Chem Sci 2018;9:1112–8.
[39] Jourden JLM, Daniel KB, Cohen SM. Chem Commun 2011;47:7968–70.
[40] Gong YJ, Feng DD, Zhang YP, Liu WN, Feng S, Zhang G. Talanta 2021;224:121785.